

Quantum Effect on the Energy Levels of Eu^{2+} Doped $\text{K}_2\text{Ca}_2(\text{SO}_4)_3$ Nanoparticles

Numan Salah · Sami S. Habib · Zishan H. Khan

Received: 9 July 2009 / Accepted: 23 March 2010 / Published online: 13 April 2010
© Springer Science+Business Media, LLC 2010

Abstract Quantum confinement effect on the energy levels of Eu^{2+} doped $\text{K}_2\text{Ca}_2(\text{SO}_4)_3$ nanoparticles has been observed. The broad photoluminescence (PL) emission band of Eu^{2+} doped $\text{K}_2\text{Ca}_2(\text{SO}_4)_3$ microcrystalline sample observed at ~436 nm is found to split into two narrow well resolved bands, located at 422 and 445 nm in the nanostructure form of this material. This has been attributed to the reduction in the crystal field strength of the nanomaterials, which results in widening the energy band gap and splitting the broad $4f^65d$ energy level of Eu^{2+} . Energy band gap values of the micro and nanocrystalline $\text{K}_2\text{Ca}_2(\text{SO}_4)_3$ samples were also determined by measuring the UV–visible absorption spectra. These values are 3.34 and 3.44 eV for the micro and nanocrystalline samples, respectively. These remarkable results suggest that activators having wide emission bands might be subjected to weak crystal strength via nanostructure materials to modify their electronic transitions. This might prove a powerful technique for producing new-advanced materials for use in the fields of solid state lasers and optoelectronic devices.

Keywords Quantum confinements · Nanoparticles · Eu^{2+} · $\text{K}_2\text{Ca}_2(\text{SO}_4)_3$ · Quantum dots · Photoluminescence

Introduction

In the last 18 years, research in nanoscience and nanotechnology has become an increasingly active field of interna-

tional interest. Nanostructure materials have attracted many workers in various fields from material science to biotechnology and genetics [1–4]. Many more nanomaterials are finding applications in diverse fields [5–7]. A number of physical phenomena become noticeably pronounced as the size of the system decreases. These include quantum mechanical effects, for example the “quantum size effect” where the electronic properties of solids are altered with great reductions in particle size. This effect does not come into play by going from macro to micro dimensions. However, it becomes dominant when the nanometer size range is reached. Materials reduced to the nanoscale can suddenly show very different properties compared to what they exhibit on a macroscale, enabling unique applications.

Effect of particle size on the optical properties has been observed by several investigators [8–14]. Reducing the particle size to a nanoscale is expected to be associated with substantial changes in the electrons configurations due to the change in the positions of their energy levels. The optical properties of different materials are more probable to be effected by reducing their particle size. Several authors have reported on the observation of blue/red shifts and appearance/disappearance of some emission bands, while going to nanostructure materials [8, 9, 15–18]. However, the actual mechanisms are not well understood. The studies on such phenomena have not been done sufficiently.

Europium (Eu) is a well-known activator, widely used in a red phosphor in television sets and fluorescent lamps, and as an activator for yttrium-based phosphors [19]. Europium doped plastics and some types of glass are used as laser materials [20]. Trivalent europium)Eu³⁺) gives red phosphors, while divalent europium (Eu²⁺) gives blue phosphors. The two europium phosphor classes, combined with the yellow/green terbium phosphors, give the “trichromatic” lights that are becoming so important to provide economical

N. Salah (✉) · S. S. Habib · Z. H. Khan
Center of Nanotechnology, King Abdulaziz University,
Jeddah 21589, Saudi Arabia
e-mail: nsalah@kau.edu.sa
e-mail: alnumany@yahoo.com

lighting. Divalent europium (Eu^{2+}) has ionic radius ~ 0.117 nm [21], when doped with microcrystalline materials, it mostly shows broad emission bands due to the transition from its broad energy level $4f^65d$ to $^8S_{7/2}$ [9, 19, 21, 22]. The position of this emission band varies from host to host.

Langbeinite are minerals with chemical formula $\text{Me}_2^+\text{Me}_2^{2+}(\text{SO}_4)_3$ where $\text{Me}^+ = \text{K, Rb, Tl, Cs or NH}_4$ and $\text{Me}^{2+} = \text{Mg, Ni, Co, Zn, Fe, Mn, Cd or Ca}$. Recently, interest in langbeinites has been increased as some of them are found to be very good thermoluminescent dosimeter (TLD) phosphors especially when doped with suitable impurities. Sahare and Moharil [23] have doped $\text{K}_2\text{Ca}_2(\text{SO}_4)_3$ with Eu and found it to be highly sensitive TLD phosphor for γ -rays of ^{60}Co as this impurity incorporated in the host in its divalent form i. e. E^{2+} . More work on this material is still continued [24–28]. The nanostructure form of $\text{K}_2\text{Ca}_2(\text{SO}_4)_3:\text{Eu}$ was also prepared [18, 26].

It is highly desirable to initiate a detailed electronic structure investigation on a wide band emission activators incorporated in nanostructure materials as the optical properties of these activators are more probable to be modified by the crystal strength via nanostructure forms. In this work we report on the observation of energy band splitting of Eu^{2+} incorporated in the host of $\text{K}_2\text{Ca}_2(\text{SO}_4)_3$ nanoparticles. This has been observed in the photoluminescence (PL) emission spectrum of the nanostructure material. This nanomaterial was synthesized by the chemical co-perception technique and its corresponding microcrystalline sample was prepared by the solid-state diffusion method. The band gaps of the nano and microcrystalline materials were also obtained. These results have been explained and are investigated in more details.

Experimental

Nanoparticles of $\text{K}_2\text{Ca}_2(\text{SO}_4)_3:\text{Eu}$ sample was first prepared by Panday et al. [26]. They have prepared this nanomaterial

by the chemical co-perception method. In this method Europium sulfate (99.99%), calcium chloride, potassium chloride, ammonium sulfate and ethanol were of analytical reagent grade (AR) and were used without further purification. Chloride salts of calcium and potassium were dissolved in double-distilled deionized water. Water-soluble sulfate salt of europium (0.1%mol) was added to the Ca^{2+} and K^+ solution. This solution was then mixed with ammonium sulfate stoichiometrically in the presence of ethanol. The co-precipitants were filtered out and washed several times with distilled water. Nanocrystalline $\text{K}_2\text{Ca}_2(\text{SO}_4)_3:\text{Eu}$ powder was finally obtained by drying the co-precipitants for about 4 h at 353 K. The powder was annealed in a quartz boat at 1,000 K for 2 h and quenched by taking the boat out of the furnace and placing it on a metal block.

The microcrystalline sample of $\text{K}_2\text{Ca}_2(\text{SO}_4)_3:\text{Eu}$ was prepared by the solid-state diffusion method [23]. In this method, K_2SO_4 of AR grade was dissolved in triply distilled deionized water. Sulfate salt of europium (0.1 mol%) was added to this solution. Water was evaporated slowly from this solution. This was then homogeneously mixed with AR grade CaSO_4 (in the molar ratio 1:2) in an agate mortar. The mixture was then heated in silica crucible at 1,237 K for 24 h to form the compound. It was then slowly cooled to room temperature and crushed and sieved to yield particle size in the range 100–125 μm . The phosphor in microcrystalline powder form thus obtained was then annealed in quartz boat at 1,000 K for 2 h and quenched by taking the boat out of the furnace and placing it on a metal block.

Scanning electron microscope (SEM) images of $\text{K}_2\text{Ca}_2(\text{SO}_4)_3:\text{Eu}$ nanocrystalline powder were obtained on a scanning electron microscope, JEOL “JSM-6360 LV.”. Shape and size of the prepared nanocrystalline powder were determined by the SEM. The SEM images shown in Fig. 1 (a and b) is a confirmation for the nanostructure form of the prepared $\text{K}_2\text{Ca}_2(\text{SO}_4)_3:\text{Eu}$ material. The particles sizes range from 20 to 40 nm. They have a semispherical shape, which is a confirmation to our earlier results [18].

Fig. 1 SEM images of $\text{K}_2\text{Ca}_2(\text{SO}_4)_3:\text{Eu}$ nanoparticles

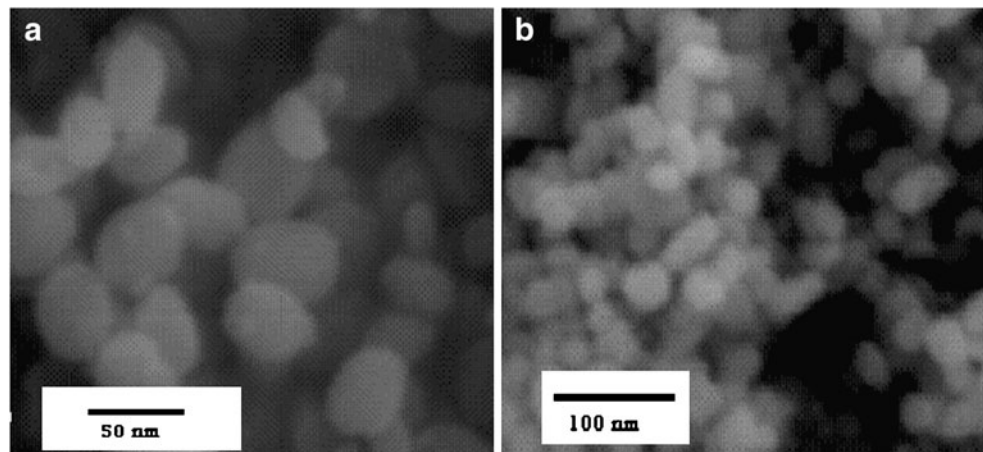
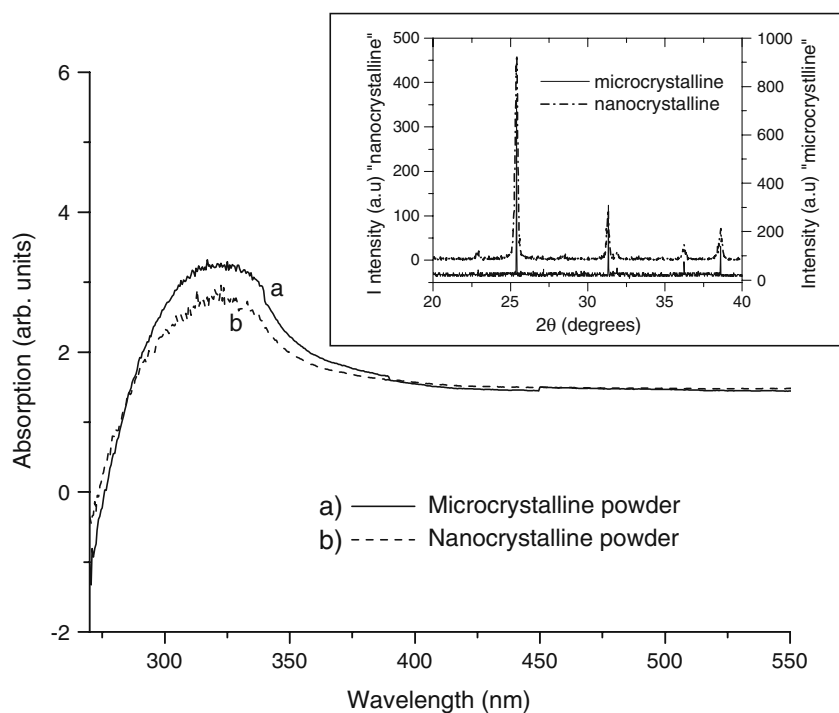


Fig. 2 UV–visible absorption spectra for the $K_2Ca_2(SO_4)_3:Eu$ micro-and nanocrystalline samples. XRD patterns are also shown in the inset



To confirm the formation of the compound, X-ray diffraction pattern was studied at room temperature for both nano- and microcrystalline samples. XRD results are studied in detail and documented earlier [29]. Those results are also shown here in the inset of Fig. 2. The band gaps of the micro and nanocrystalline materials of $K_2Ca_2(SO_4)_3$ were obtained using UV–visible absorption spectra. The measurements were carried out using U-3300 spectrophotometers (Hitachi). Photoluminescence (PL) emissions spectra of the samples were recorded using “Varian Cary Eclipse” Fluorescence Spectrophotometer (fitted with Xenon lamp) with spectral width of 2.5 nm and medium PMT detector voltage. The same amount of samples was taken every time for recording PL.

Results

Energy band gap

Figure 2 shows the optical absorption spectra of the nano and microcrystalline $K_2Ca_2(SO_4)_3$ samples near the fundamental absorption edge. The optical energy gaps E_g of the nanophosphor as well as microphosphor were calculated using Tauc relation [30–32]

$$\alpha(hv) \sim (hv - E_g)^{1/n}, \quad (1)$$

where $h\nu$ is the photon energy and α is the optical absorption coefficient near the fundamental absorption edge. The absorption coefficients α were calculated from

these optical absorption spectra. The values of the optical band gap of the micro and nanocrystalline $K_2Ca_2(SO_4)_3$ are obtained by plotting $(\alpha h\nu)^n$ versus $h\nu$ in the high absorption range followed by extrapolating the linear region of the plots to $(\alpha h\nu)^n = 0$. The analysis of the present data showed that the plots of $(\alpha h\nu)^n$ against $h\nu$ give linear relations which are the most fitted for Eq. 1 with $n=2$, for both micro and nanocrystalline samples (Fig. 3). This indicates that the allowed direct transition is responsible for the interband transitions in $K_2Ca_2(SO_4)_3$ micro and nanocrystal. The optical energy band gap for the micro and nanocrystalline $K_2Ca_2(SO_4)_3$ are found to be 3.34 and 3.44 eV, respectively.

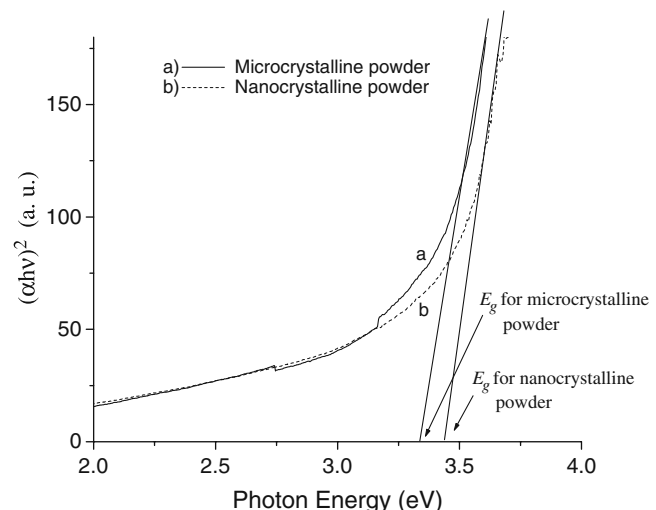


Fig. 3 Plot for $(\alpha h\nu)^2$ as a function of the incident photon energy ($h\nu$) for the $K_2Ca_2(SO_4)_3:Eu$ micro-and nanocrystalline samples

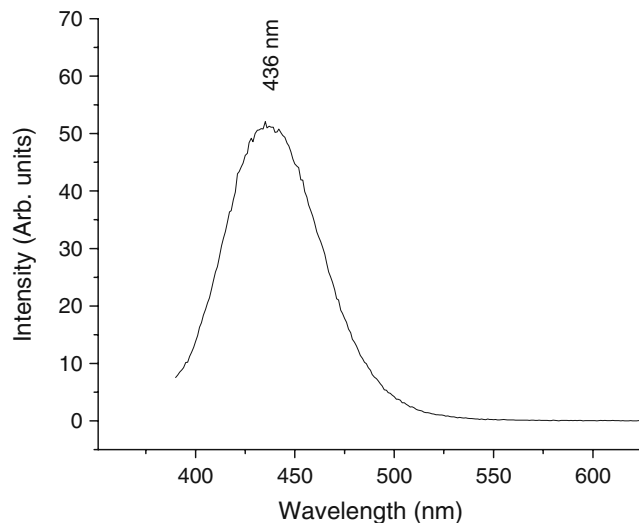


Fig. 4 PL emission spectrum of $\text{K}_2\text{Ca}_2(\text{SO}_4)_3:\text{Eu}$ microcrystalline powder

Photoluminescence (PL)

Photoluminescence (PL) emissions spectra of $\text{K}_2\text{Ca}_2(\text{SO}_4)_3:\text{Eu}$ micro and nanocrystalline samples are shown in Figs. 4 and 5, respectively. The materials were excited by 322 nm. In case of microcrystalline sample, single emission broadband is observed at around 436 nm (Fig. 4), which can be assigned to the transitions between the lowest band of the $4f^65d$ configuration and the ground state $^8S_{7/2}$ of the $4f^7$ configuration of Eu^{2+} ion. These results are matched with those reported earlier by Dhopte et al. [33, 34]. Un-like the microcrystalline sample, the nanoparticles have showed two narrow well-resolved bands located at 422 and 445 nm (Fig. 5).

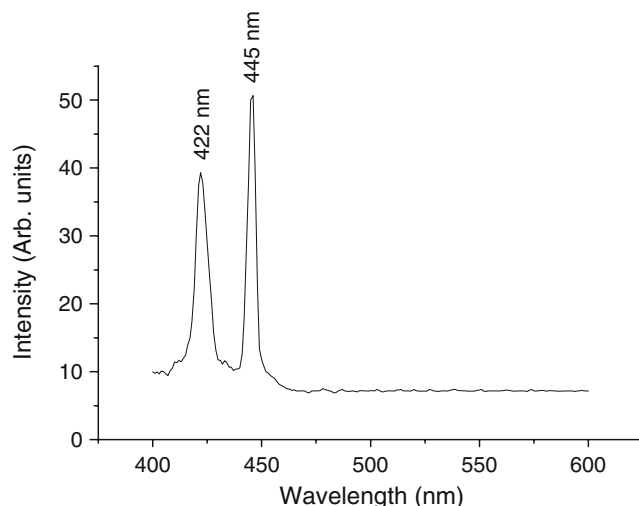


Fig. 5 PL emission spectrum of $\text{K}_2\text{Ca}_2(\text{SO}_4)_3:\text{Eu}$ nanocrystalline powder

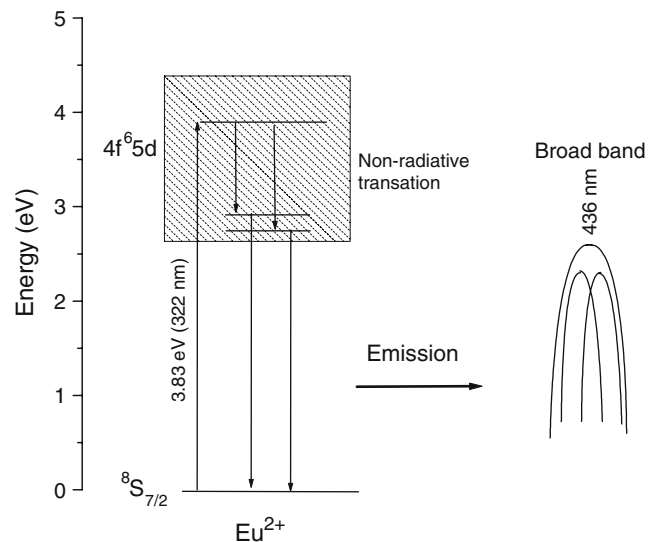


Fig. 6 Schematic energy level diagram showing the broad emission in $\text{K}_2\text{Ca}_2(\text{SO}_4)_3:\text{Eu}$ microcrystalline powder

Discussion

In the microcrystalline sample of $\text{K}_2\text{Ca}_2(\text{SO}_4)_3:\text{Eu}$, maximum PL emission is observed at ~436 nm. This emission is observed as a broad band with FWHM is around 60 nm (Fig. 4) and attributed to $4f^65d \rightarrow ^8S_{7/2}$ transition of Eu^{2+} [28]. But in the nanostructure form of this material having particles sizes in the range 20–40 nm, this broad emission band is observed as two narrow emission bands (Fig. 5), indicating the degeneracy of the broad energy level $4f^65d$ of Eu^{2+} into two discrete levels. These are $4f^65d(e_g)$ and $4f^65d(t_{2g})$ [9]. These results suggest that the $\text{K}_2\text{Ca}_2(\text{SO}_4)_3$ nanoparticles are in a quantum confinement region. This has been illustrated in Figs. 6 and 7. In the microcrystalline form, the

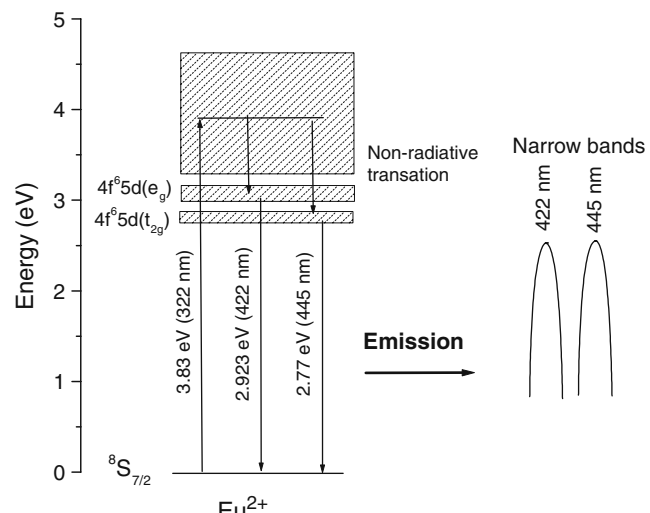


Fig. 7 Schematic energy level diagram showing the narrow emissions in $\text{K}_2\text{Ca}_2(\text{SO}_4)_3:\text{Eu}$ nanocrystalline powder

broad emission at 436 nm is proposed to be a combination of two emissions (Fig. 6), while in case of nanomaterial it get resolved into two separate emissions (Fig. 7). It is well understood that when the size of the nanocrystals decreases to the exciton Bohr diameters, the energy level develops discrete levels from the continuum, and the energy gap increases, showing a quantum confinement effect [8, 11, 14, 35, 36]. This was reported to exist in “quantum dots” [14] where the particle size is mostly less than 10 nm. It has been attributed to the widening of the energy band gap of the nanomaterials due the decrease of the crystal strength effect [35–38]. However, quantum confinement effect might occur at particle size greater than Bohr diameter as observed by Lee et al. in ZnCdSe nanocrystals [10]. In the present $K_2Ca_2(SO_4)_3:Eu^{2+}$ nanoparticles, this effect seems to occur at particle size >20 nm. Reducing the particle size to a nanoscale (Fig. 1) results in widening the band gap by around 0.1 eV (Fig. 3). This might be due to the drastic decreases in the crystal field strength, which reflects on degeneration of the broad energy level $4f^65d$ of Eu^{2+} .

The PL result presented here for $K_2Ca_2(SO_4)_3:Eu^{2+}$ nanomaterial is very remarkable. Pandey et al. [26] were studied this material as a TLD. They also have studied the PL emission of this material excited by a He–Cd Laser with 325 nm excitation wavelength. In their results, the emission spectrum contained two bands around 400 and 450 nm. They have speculated that both the bands correspond to the Eu^{2+} emission arising due to transitions between the lowest band of the $4f^65d$ configuration and the ground state $^8S_{7/2}$ of the $4f^7$ configuration of Eu^{2+} ion, but with Eu^{2+} occupying two different lattice sites (i.e., Eu^{2+} substituting K^+ ions in the host lattice may lead to emission around 450 nm while that substituting Ca^{2+} may give emission around 400 nm). However, effect of particle size on these emissions was not investigated by Pandey et al. [26]. In the present nanomaterial the same procedure was used for synthesizing the nanomaterials. But, the PL emissions in the present nanomaterials are observed to be narrower (emissions at 422 and 445 nm) than those observed by Pandey et al. [26] with a slight change in the position of these emission bands. These differences between our and their results are might be due to the use of different excitation sources and PMT detectors having different resolution power. In another work [18] when we have changed the initial compound of Eu^{2+} using chloride salt instead of sulfate salt, there was only a single emission at 384 nm. It means that there are several factors are responsible for the electronic transitions in the materials beside the particle size effect. Nature of the initial materials is found to play a significant role in these transitions [18]. Sensitivity and resolution of the detectors beside the experience of the user are also critical parameters for observing the real and actual emissions.

In other materials, several authors have reported on the observation of red shifted emission bands, while going to nanostructure materials [10, 12, 13]. On the view of their results and our presented results we might proposed that there will not be any red shift in the energy levels while going from bulk/micro to nanoscale materials, since there will always be a decrease in the crystal field strength. The energy levels of different materials are going to face the same effect and show a shift (if any) in the emission bands in one direction, which is the blue direction. Moreover, the electrons at the discrete energy levels in case of the nanomaterials are not necessarily having the same quantum numbers and electronic transitions probabilities as they have in bulk/micro materials. Due to the reorganization of the energy levels, the quantum numbers of the electrons at these levels might be changed. For example the spin quantum number of an electron at the discrete energy level of the nanomaterial should not necessary remains the same as it was in case of bulk material. In other words going from bulk/micro to nanostructured materials, there is a probability for some allowed transitions to become forbidden and vice versa. Spin–orbit interactions are going to be changed due to the reorganization of these energy levels in the nanostructure materials. Therefore the emissions that observed to be red shifted might be a result of completely new transitions between new energy levels, which are property of the nanostructured materials. There is a possibility for a slight blue shift in the emission bands, while going from bulk/micro to nanostructure materials. But in some materials there will not be just shifts or appearance/disappearance of emission bands; there might be substantial changes in the electrons wave functions and transitions probabilities. Different studies showed that there is a missing of some emissions and an appearance of some others. This has been observed in a large number of experiments. But the authors could not recognize the actual mechanism. For example Yan et al. [9] have reported on a missing of some transitions in Eu^{2+} doped $KMgF$ nanoparticles. They have reported on a missing of the band at 420 nm while going from single crystal to nanoparticles with appearance of a single sharp emission band at 360 nm. They also have mentioned a blue shift in the excitation spectrum of the nanoparticles by around 70 nm compared with that of the $KMgF:Eu^{2+}$ single crystal. Quantum size effect caused by the formation of small nanoparticles was pronounced in these materials as mentioned by Yan et al. [9]. This results in splitting the energy level $4f^65d$ of Eu^{2+} into the $4f^65d(e_g)$ and $4f^65d$ levels. However, all these observations mentioned by Yan et al. [9] indicate that there are substantial changes in the electrons configurations, changing their wave functions and transitions probabilities. Missing the band at 420 nm of Eu^{2+} in $KMgF:Eu^{2+}$ means that this transition becomes forbidden. Due to a slight shift in the energy levels of Eu^{2+} in these nano-

materials, the spin quantum numbers of the electrons at these levels, which may have a responsibility for the allowed/forbidden transitions, might change, resulting in completely new transitions (By means spin–orbit interactions). Even the sharp band appeared at 360 nm in the nanocrystals [9], might not be a property of the original energy level (In bulk structure); it might be due to newly allowed transition from another energy level in the nanostructure material. This might be a new emission representing transition from one of the discrete levels that has acquired new quantum numbers. At these contexts, there will be drastic changes in the optical, electrical and magnetic properties of the materials at their nanostructure forms.

Measurement of the emission spectra of the nano-materials that shows quantum confinement effects is a very critical step, requires experts worker in this field. For example Chen et al. [37] have studied the size effect on the fluorescence of Eu²⁺ in ZnS nanoparticles. They claimed that the emission bands of the 4.2, 3.2 and 2.6 nm sized ZnS:Eu²⁺ nanoparticles are peaking at 670, 580 and 520 nm, respectively. They have attributed the blue shift to the crystal strength effect and to the decreases in the electron–phonon coupling. Our view in this point is that this wide shift by around 150 nm while going from 4.2 nm to 2.6 nm is not due to the above-mentioned reasons given by the authors. They should notice that there would not be a huge shift in the emission bands with changing the particle size in a very small range. Probably these different results are due to the use of different initial materials to get different sizes. The Initial materials are playing a major role in the optical properties [18]. Moreover, in their TEM image there is no appearance for single nanoparticles in the range of few nanometers as claimed by the authors. The material might not have a nanostructure form at all.

From the application point of view, formulating the materials in the nanoscale size is a powerful technique for annihilating/generating emission bands of some activators. Our finding here might has its importance in the fields of laser materials and optoelectronic devices. Subjecting wide emission band activators like Eu²⁺ to weak crystal field via nano-structure materials may become the method of choice for fabricating high-power lasers. Due to the possible change in the spin–orbit interactions, we might be able to modify the optical, electrical and magnetic properties of different materials. Via this approach we may add a new superiority for the nanomaterials and nanotechnology leading to novel advanced materials with different properties than conventional materials.

Conclusions

Quantum confinement effect on the energy levels of Eu²⁺ doped K₂Ca₂(SO₄)₃ nanoparticles has been observed. The

broad emission band of Eu²⁺ observed at 436 nm in the microcrystalline form of this sample is found to split into two narrow well-resolved bands located at 422 and 445 nm. This has been attributed to the reduction of the crystal field strength. On the view of these results we might conclude that: (1) Quantum Confinement effect is not limited to particles with sizes bellow 10 nm (2) The wave functions and transition probabilities of the electrons might be changing while going from bulk/micro to nanostructure materials (3) The wide emission bands of some activators such as Eu²⁺ are more probable to be effected by the size of the particles (4) the nature of the initial compounds forming the nanostructure materials has a significant role in the optical properties of the materials. Considering these conclusions, we might be able to formulate novel advanced laser and other nanomaterials with different properties than conventional materials.

Acknowledgments The authors are thankful to Dr. Salem, Department of Biological Science, KAU for taking SEM images.

References

1. Fonseca A, Franco N, Alves E, Barradas NP, Leitão JP, Sobolev NA, Banhart DF, Presting H, Ulyanov VV, Nikiforov AI (2005) Nucl Instrum Methods B 241:454
2. Freitas MLL, Silva LP, Azevedo RB, Garcia VAP, Lacava LM, Grisolia CK, Lucci CM, Morais PC, Da Silva F, Buske N, Curi R, Lacava ZGM (2002) J Magn Magn Mater 252:396
3. Kerman K, Morita Y, Yuzuru T, Ozsoz M, Eiichi T (2004) Anal Chim Acta 510:169
4. Locher CP, Putnam D, Langer R, Witt SA, Ashlock BM, Levy JA (2003) Immunol Lett 90:67
5. Xu NS, Ejaz Huq S (2005) Mater Sci Eng R 48:47
6. Lindgren T, Mwabora JM, Avendaño E, Jonsson J, Hoel A, Granqvist CG, Lindquist S-E (2003) J Phys Chem B 107:5709
7. Rodríguez J, Gómez M, Niklasson GA, Lindquist S-E, Granqvist CG (2001) J Mater Sci 36:3699
8. Susmita K, Sunirmal J, Biswas KP, (2005) Mater Sci-Poland, 23
9. Yan J-h, Zhang M, Lian H-z, Liu J, Li Z-t, Cao J, Shi Cs (2006) Chem Res Chin Univ 22:247
10. Lee H, Yang H, Holloway PH (2007) J Lumin 126:314
11. Sharmaa SN, Kohli S, Rastogi AC (2005) Physica E 25:554
12. Chang HJ, Lu CZ, Wang Y, Son C-S, Choi I-H (2004) J Korean Phys Soc 45:959
13. Liu CM, Guo L, Xu HB, Wu ZY, Weber J (2003) Microelectron Eng 66:107
14. Jeang E-H, Lee J-H, Je K-C, Yim S-Y, Park S-H, Choi Y-S, Choi J-G, Treguer M, Thierry C (2004) Bull Korean Chem Soc 25:934
15. Nakaema MKK, Brasil MJSP, Iikawa F, Ribeiro E, Heinzel T, Ensslin K, Medeiros-Ribeiro G, Petroff PM, Brum JA (2002) Physica E Low dimens Syst Nanostruct 12:872
16. Djurić AB, Leung YH, Tam KH, Ding L, Ge WK, Chen HY, Gew S (2006) Appl Phys Lett 88:103–107
17. Larcheri S, Armellini C, Rocca F, Kuzmin A, Kalendarev R, Dalba G, Graziola R, Purans J, Pailharey D, Jandard F (2006) Superlattices Microstruct 39:267
18. Salah N, Lochab SP, Ranjan R, Kanjilal D, Habib SS, Aleynikov VE, Rupasov AA (2007) J Appl Phys 102:64904

19. Sung H-J, Ko K-Y, Hyun SK, Kweon S-S, Park J-Y, Do YR, Huh Y-D (2006) Bull Korean Chem Soc 27:841
20. Nakamura K, Hasegawa Y, Wada Y, Shozo Y (2004) Chem Phys Lett 398:500
21. Salah N, Sahare PD, Kumar P (2006) Phys Status Solidi A 203:898
22. Fox PJ, Akber RA, Prescott RJ (1981) J Phys D 21:189
23. Sahare PD, Moharil SV (1990) J Phys D 23:567
24. Stochioiu A, Georgescu I (2003) Rom Rep Phys 55:136
25. Pandey A, Sharma VK, Mohan D, Kale RK, Sahare PD (2002) J Phys D 35:1330
26. Pandey A, Sonkawade RG, Sahare PD (2002) J Phys D 35:2744
27. Sahare PD, Salah N, Lochab SP, Mohanty T, Kanjilal D (2005) J Phys D 38:3995
28. Salah N, Sahare PD (2006) Radiat Meas 41:665
29. Salah N, Sahare PD, Nawaz S, Lochab SP (2004) Radiat Eff Defects Solid 159:321
30. Tauc J (1970) In: Abeles F (ed) Optical properties of solids. North-Holland, Amsterdam
31. Pankove JJ (1971) Optical process in semiconductors. Dover, New York, p 39
32. Sze SM (2004) Physics of semiconductor devices, 2nd edn. Wiley, New York, p 39
33. Dhopte SM, Muhal PL, Kondawar VK, Moharil SV, Sahare PD (1991) J Phys D 24:1869
34. Blasse G, Grabmaier C (1994) Luminescent materials. Springer-Verlag, Germany, Chap 3
35. Gong X, Wu P, Chan WK, Chen W (2000) J Phys Chem Solids 61:115
36. Moriarty P (2001) Rep Prog Phys 64:297
37. Chen W, Malm JO, Zwiller V, Wallenberg R, Bovin JO (2001) J Appl Phys 89:2671
38. Chen W, Sammynaiken R, Huang YN, Malm JO, Wallenberg R, Bovin JO, Zwiller V, Kotov NA (2001) J Appl Phys 89:1120